



**HAL**  
open science

## Improved Power Factor in Self-Substituted Fe<sub>2</sub>VAl Thermoelectric Thin Films Prepared by Co-sputtering

Daniel Bourgault, Hajar Hajoum, Sébastien Pairis, Olivier Leynaud, Richard Haettel, Jean François Motte, Olivier Rouleau, Eric Alleno

► **To cite this version:**

Daniel Bourgault, Hajar Hajoum, Sébastien Pairis, Olivier Leynaud, Richard Haettel, et al.. Improved Power Factor in Self-Substituted Fe<sub>2</sub>VAl Thermoelectric Thin Films Prepared by Co-sputtering. ACS Applied Energy Materials, 2023, 6 (3), pp.1526-1532. 10.1021/acsaem.2c03405 . hal-03948872

**HAL Id: hal-03948872**

**<https://hal.science/hal-03948872>**

Submitted on 20 Jan 2023

**HAL** is a multi-disciplinary open access archive for the deposit and dissemination of scientific research documents, whether they are published or not. The documents may come from teaching and research institutions in France or abroad, or from public or private research centers.

L'archive ouverte pluridisciplinaire **HAL**, est destinée au dépôt et à la diffusion de documents scientifiques de niveau recherche, publiés ou non, émanant des établissements d'enseignement et de recherche français ou étrangers, des laboratoires publics ou privés.

# Improved power factor in self-substituted Fe<sub>2</sub>VAl thermoelectric thin films prepared by co-sputtering

Daniel Bourgault<sup>\*(1,2)</sup>, Hajar Hajoum<sup>(1,2)</sup>, Sébastien Pairis<sup>(1,2)</sup>, Olivier Leynaud<sup>(1,2)</sup>, Richard Haettel<sup>(1,2)</sup>, Jean François Motte<sup>(1,2)</sup>, Olivier Rouleau<sup>(3)</sup>, Eric Alleno<sup>(3)</sup>

<sup>(1)</sup> Univ. Grenoble Alpes, Institut Néel, F-38042 Grenoble, France.

<sup>(2)</sup> Centre National de la Recherche Scientifique / Institut Néel, 25 Avenue des Martyrs,  
BP 166, 38042 Grenoble Cedex 9, France

<sup>(3)</sup> Univ. Paris Est Creteil, CNRS, ICMPE, UMR 7182, 2-8, rue H. Dunant, F-94320 Thiais,  
France

\* Corresponding author ; E-mail : [daniel.bourgault@neel.cnrs.fr](mailto:daniel.bourgault@neel.cnrs.fr)

Keywords : Thermoelectric, thin film, Fe<sub>2</sub>VAl, High power factor, co sputtering

## Abstract

We present a strong improvement of the electronic transport properties in the Fe<sub>2</sub>VAl Heusler alloy obtained in thin film form by a co-sputtering process. The power factor is improved when deposition occurs at temperatures close to 873 K and when composition is tuned using a co-sputtering process. High values up to 5.6 mW/K<sup>2</sup>m are obtained for *n*-type films deposited at 873 K which is up to now a record for self-substituted Fe<sub>2</sub>VAl thermoelectric thin films. Influence of the co-sputtering conditions on atomic composition as well as substrate effect on electronic transport properties are also presented.

## 1-Introduction

Fe<sub>2</sub>VAl-based full-Heusler alloy is a promising material for thermoelectric applications. In such devices, a high figure of merit  $ZT$  is required to increase conversion efficiency. The figure of merit is expressed by  $ZT = (S^2/\rho\lambda)T$ , where  $S$ ,  $\rho$ ,  $\lambda$ , and  $T$  are respectively the Seebeck coefficient, electrical resistivity, thermal conductivity, and absolute temperature. Fe<sub>2</sub>VAl alloy shows high  $S$  when the valence electron concentration (VEC) per atom is close to 6.<sup>1,2</sup> Miyazaki et al.<sup>3</sup> and Diack-Rasselio et al.<sup>4</sup> also observed that the thermoelectric power factor ( $P_F = S^2/\rho$ ) is enhanced in  $n$ -type off-stoichiometric Fe<sub>2-x</sub>V<sub>1+x</sub>Al bulk alloys ( $x \sim 0.03 - 0.05$ ). The highest power factors  $P_F = 7.6 \text{ mW/K}^2\text{m}$ <sup>5</sup> and  $6.7 \text{ mW/K}^2\text{m}$ <sup>6</sup> at room temperature are larger for such alloys than that of Bi<sub>2</sub>Te<sub>3</sub> materials. However, the figure of merit ( $ZT \sim 0.1$  at 300 K) is lower than that of Bi<sub>2</sub>Te<sub>3</sub> compounds because of its high lattice thermal conductivity ( $\lambda_L$ ) of about 20 W/(m·K). This is due to a relatively large Debye temperature ( $\theta_D = 540 \text{ K}$ ) and sound velocity ( $v = 4150 \text{ m s}^{-1}$ ).<sup>7</sup> By substituting heavy chemical elements (see reference<sup>8</sup>) such as Ta for instance<sup>9</sup>, the induced atomic mass fluctuations lead to a decrease of  $\lambda_L$ , and to an increase of  $ZT$  to 0.2 at 400 K. By decreasing the average grain size to around 100 nm to scatter the phonons on the numerous grain boundaries, the thermal conductivity could be further reduced to  $4.5 \text{ W/(m·K)}$ <sup>10</sup> and  $ZT$  increased to  $ZT = 0.3$  at 500 K.

The sputtering method has been mainly used for the development of full-Heusler Fe-V-Al thin films<sup>11-17</sup> and epitaxied Fe<sub>2</sub>VAl/W and Fe<sub>2</sub>VAl/Mo superlattices.<sup>18</sup> Molecular beam epitaxy (MBE) techniques were also implemented, leading to Fe<sub>2</sub>VAl epitaxial films with a high crystallinity and a stoichiometric chemical composition.<sup>19,20</sup> Such studies mainly aimed at taking benefits of the thin film or superlattice forms to reach low thermal conductivity values such as  $\lambda = 4 \text{ W m}^{-1} \text{ K}^{-1}$  in ref.<sup>13,15,18,20</sup>. However, high power factor value could not be reach, except in ref.<sup>11</sup> where  $P_F$  was improved to  $3.0 \text{ mW/K}^2\text{m}$  in Fe<sub>1.93</sub>V<sub>1.05</sub>Al<sub>0.77</sub>Si<sub>0.24</sub>. Nonetheless, this last value doesn't exceed half the maximum value obtained in bulk  $n$ -type Fe<sub>2</sub>VAl.

Recently, B. Hinterleitner et al. reported an exceptionally large  $ZT$  of 6 at 380 K in a Fe<sub>2</sub>V<sub>0.8</sub>W<sub>0.2</sub>Al thin film.<sup>21</sup> This value is two orders of magnitude larger than bulk Fe<sub>2</sub>V<sub>0.9</sub>W<sub>0.1</sub>Al synthesized by Mikami et al..<sup>22</sup> This high figure of merit is attributed to a large Seebeck coefficient of  $-550 \text{ } \mu\text{V/K}$  measured by the authors. Combined to a small value of electrical resistivity ( $\rho = 0.6 \text{ m}\Omega \text{ cm}$ ), this leads to an unexpectedly large power factor  $P_F =$

50 mW/K<sup>2</sup>m. Such result would mean a great progress for the thermoelectric community, but this experimental result has been theoretically discussed<sup>8</sup> and has not yet been experimentally reproduced by another research group. Consequently, research to improve the  $ZT$  and primarily the power factor of Fe-V-Al films needs to be pursued.

Thermoelectrical properties of Fe-V-Al thin films being very sensitive to the composition, we studied their elaboration using a co-sputtering process based on a Fe<sub>2</sub>VAl primary target and a secondary V or Al target. Composition tuning was thereby enabled by the co-sputtering process, yielding to  $n$ -type and  $p$ -type thin films with very encouraging electronic transport properties.

## 2-Experimental section

Starting from stoichiometric alloys prepared by induction melting, a Fe<sub>2</sub>VAl target of 50 mm in diameter and 3 mm in thickness was cut using an electro-erosion process.

Magnetron sputtering deposition was achieved using ternary Fe<sub>2</sub>VAl as the principal target. A secondary target of V or Al was also used during deposition to finely tune the film composition. (001) oriented MgO single crystal was used as substrate because the MgO lattice parameter fit very well with those of Fe<sub>2</sub>VAl. Lattice mismatch between Fe<sub>2</sub>VAl and MgO is smaller than 4%. In addition, it allows quantitative composition analysis by Energy Dispersive X-ray spectroscopy (EDX) analysis and is electrically insulating for transport measurements. The DC (Direct Current) power applied to the principal ternary target was tuned to 135 W. The power of the secondary targets was varied from 0 to 28 W for V target and from 0 to 34 W for the Al target. Deposition occurred at temperatures between 733 and 873 K during 60 minutes, resulting in Fe-V-Al film thicknesses ranging from 450 to 600 nm. Sputtering was performed with an argon pressure of 10<sup>-2</sup> mbar (with a 40 Standard Cubic Centimeters per minutes (sccm) gas flowing). The target-to-substrate distance was fixed to 13 cm and the substrate holder rotation to 4 rpm to ensure chemical and temperature homogeneity for a constant film thickness.

The crystalline structure was investigated with an X-Ray Diffraction (XRD) system (D5000 Bruker) in the conventional  $\Theta$ - $2\Theta$  mode using a Cu K $\alpha$  radiation source. Film composition and microstructure images were obtained by EDX analysis and using a Zeiss Ultra + Field Emission Scanning Electron Microscope (FESEM). Film homogeneity was verified by analyzing several spots along the film.

After deposition, some films were annealed in Ar atmosphere at various temperatures up to 1023 K and for various durations up to 72 h.

The power factor  $P_F = S^2/\rho$  at room temperature was obtained by measuring the Seebeck coefficient  $S$  ( $\mu\text{V/K}$ ) and the electrical resistivity  $\rho$  ( $\text{m}\Omega \text{ cm}$ ). This factor is indicative of the output power produced by a generator, whereas the figure of merit  $ZT = (S^2/\rho\lambda)T = P_FT/\lambda$  ( $\lambda$  being the thermal conductivity) is indicative of its efficiency. A home-made device described in reference <sup>23</sup> was used to measure the Seebeck coefficient by applying a thermal gradient along the film plane. The right part of the device was maintained at room temperature (RT) while the temperature of left part was regulated using a heating cartridge up to 313 K above RT. A mechanical pressure was used to ensure good thermal and electrical contacts at the hot and cold ends of the set-up. The temperature gradient was measured with an accuracy of  $\pm 1$  K by two K-type thermocouples (0.1 mm diameter) pressed against the film surface. The induced voltage was measured using an Agilent 34401A Digital multimeter. A Jandel 4-probe (Jandel Engineering, Ltd., Bedfordshire, U.K.) was used to determine the electrical resistivity of the films. Film thickness was measured using a mechanical profilometer (See Figure S1 in Supporting Information). The charge carrier density at 300 K was obtained from Hall resistivity measurements in the 0 - 7 T range using a Van der Pauw measurement setup for thin films.

### 3-Results

#### 3.1 Influence of the co-sputtering process on atomic composition

EDX analysis leads to  $\text{Fe}_{52}\text{V}_{24.5}\text{Al}_{23.5}$  (or  $\text{Fe}_{2.08}\text{V}_{0.98}\text{Al}_{0.94}$ ) film composition without secondary target. Figure 1 displays the composition variation according to the power of the secondary Al (Figure 1a) and V (Figure 1b) targets for films deposited at a temperature of 733 K. There is a linear variation of the atomic composition in agreement with the nature and the power applied to the secondary target. Film composition can be accurately tuned by the co-sputtering process from the near-stoichiometric composition  $\text{Fe}_{50.2}\text{V}_{24.8}\text{Al}_{25}$  ( $\text{Fe}_{2.01}\text{V}_{0.99}\text{Al}$ ) to Al-rich  $\text{Fe}_{47.4}\text{V}_{22.1}\text{Al}_{30.5}$  ( $\text{Fe}_{1.90}\text{V}_{0.88}\text{Al}_{1.22}$ ) and to V-rich  $\text{Fe}_{47.6}\text{V}_{30.9}\text{Al}_{21.5}$  ( $\text{Fe}_{1.90}\text{V}_{1.24}\text{Al}_{0.86}$ ).

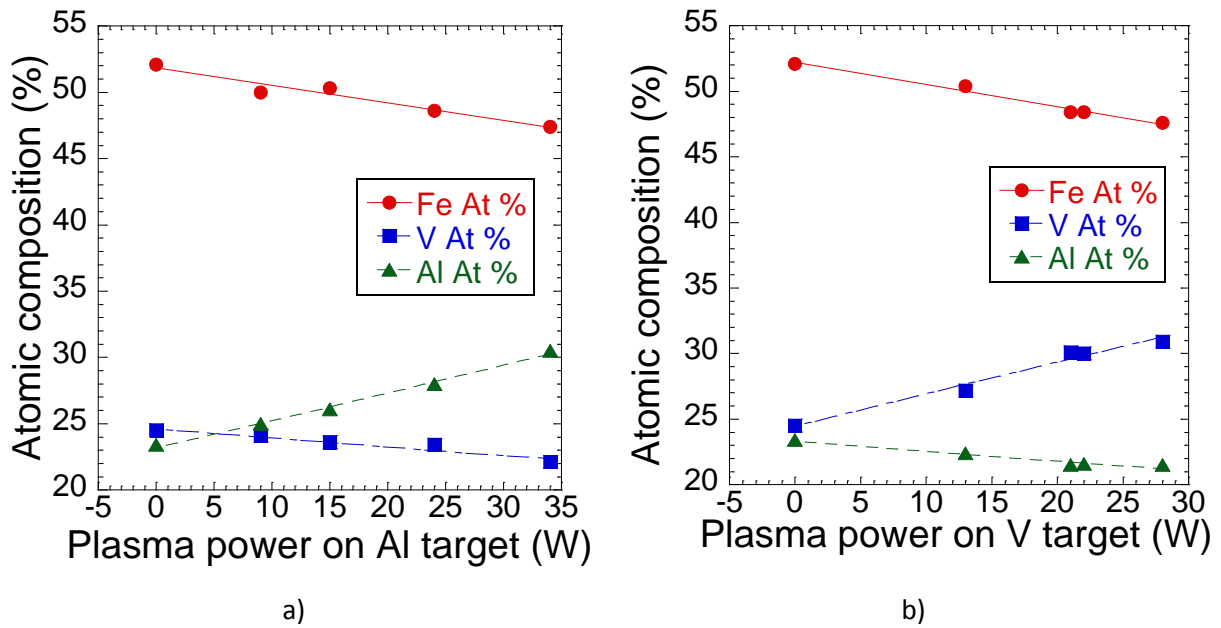


**Figure 1 : Fe, Al and V atomic concentrations determined by EDX analysis for plasma power applied to the Al (a) and V (b) target. Temperature deposition is 733 K.**

Figure 2a shows X ray diffraction patterns of Fe-V-Al films deposited at 733 K on MgO substrates for a zero-plasma power (figure 2a). The detection restricted to  $(2n\ 0\ 0)$  peaks of the Heusler structure indicates that these samples deposited on a MgO  $(1\ 0\ 0)$  substrate maintain a single-axis orientation for their crystalline structure. The occurrence of these peaks excludes the fully disordered  $A2$  structure and shows that they crystallize at least in the partially ordered  $B2$  structure. The  $(1\ 1\ 1)$  peak located near  $27^\circ$  in  $2\Theta$  corresponding to the  $L2_1$  structure is not visible in the various patterns (inset in figure 2a). The high degree of film orientation would not exhibit the  $(1\ 1\ 1)$  line characteristic of the fully ordered  $L2_1$  structure anyway even if they would crystallize in this last structure. It is thus impossible to conclude on the exact nature these film structures.

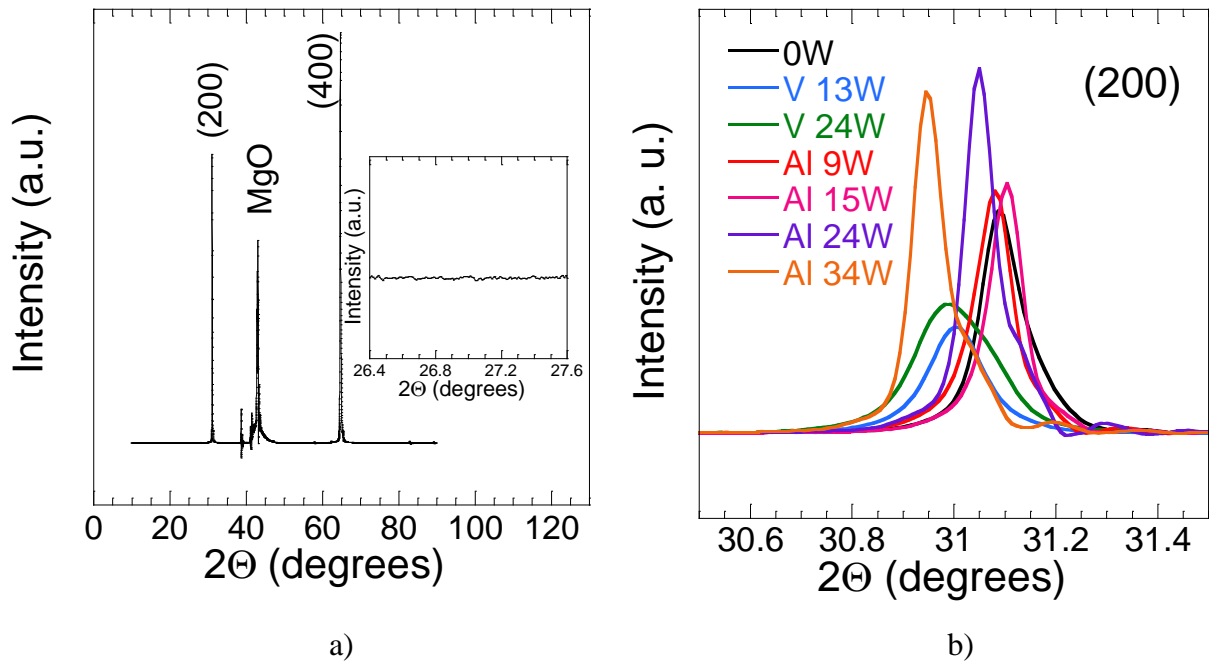


**Figure 2 : X ray diffraction patterns of Fe-V-Al films deposited at 733 K on MgO substrates for zero-plasma (a) and for various plasma power applied to the secondary V and Al targets (b). In inset of figure 2a is shown the pattern in the range of 26.4 - 27.6 degrees.**

Figure 2b shows a magnification (30.5 - 31.5° angle range) of the X ray diffraction patterns of Fe-V-Al films deposited for various plasma power applied to the secondary V and Al targets. Differences are observed in relative intensities and in full width at half-maximum (FWHM) of the (200) lines. These differences are related to the degree of epitaxy and grain size of the films deposited on MgO, which vary with film composition. It seems that Al-rich films are better epitaxied with large grains than V-rich films. By increasing aluminum or vanadium concentration we also observe a peak shift in the patterns. It reveals composition impact on the lattice parameter, which can be better seen in figure 3 where the lattice parameter is plotted as a function of the V/Al ratio. The lattice parameter increases linearly when moving away from the ratio V/Al = 1 and varies from 5.745 to 5.775 Å. This variation of the lattice parameter has already been reported in the literature<sup>3,4,24,25</sup> but is not explained by the atomic radii differences between vanadium (135 pm) and aluminum (125 pm), nor by the valence electrons concentration. Based on DFT calculations and a Bader analysis, Diack-Rasselio et al. recently demonstrated that  $Fe_2VAl$  could be seen as a “charge transfer” compound ( $Fe_2^{1.3-}V^{0.8+}Al^{1.8+}$ ) where such unusual lattice parameter variation occurring with

the V/Al ratio change in the  $\text{Fe}_2\text{V}_{1+x}\text{Al}_{1-x}$  series, could be due to these interatomic charge transfer variations.<sup>4</sup>

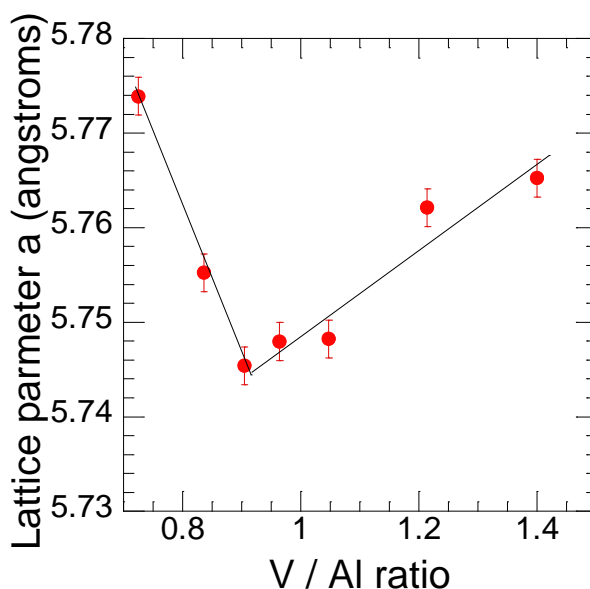


**Figure 3 : Lattice parameter for various vanadium-aluminum ratio V/Al.**

### 3.2 Seebeck coefficient and electrical resistivity versus valence electron concentration

As shown in figure 4a, the Seebeck coefficient is correlated to valence electron concentration ( $VEC$ ), which can be calculated from the measured film composition for films deposited at 733 and 873 K. The  $VEC$  value gradually increases from 5.81 to 6.10 due to film composition variation. This  $VEC$  variation around 6 enables chemical potential optimization to increase the Seebeck coefficient. For samples deposited with the secondary aluminum target, the  $VEC$  is lower than 6 and the Seebeck coefficient increases from +36  $\mu\text{V}/\text{K}$  to +68  $\mu\text{V}/\text{K}$  in these  $p$ -type thin films. For  $VEC \geq 6$  (when using the secondary vanadium target), films become  $n$ -type with  $S$  values ranging from -48  $\mu\text{V}/\text{K}$  to -97  $\mu\text{V}/\text{K}$ . The variations of  $S$  with  $VEC$  are similar for both deposition temperatures. Nonetheless, larger  $S$  values are reached for both type of conduction when depositing at 873 K rather than at 733 K.

Electrical resistivity values obtained at 300K are overall lower for thin films deposited at 873 K than at 733 K (Figure 4b). The better growth quality at 873 K (see Fig. S2 in S.I.) allows electrical resistivity values measured at 300K as low as 0.1  $\text{m}\Omega\text{-cm}$  for  $n$ -type thin films whereas it varies between 0.25 and 1  $\text{m}\Omega\text{-cm}$  for  $p$ -type thin films.

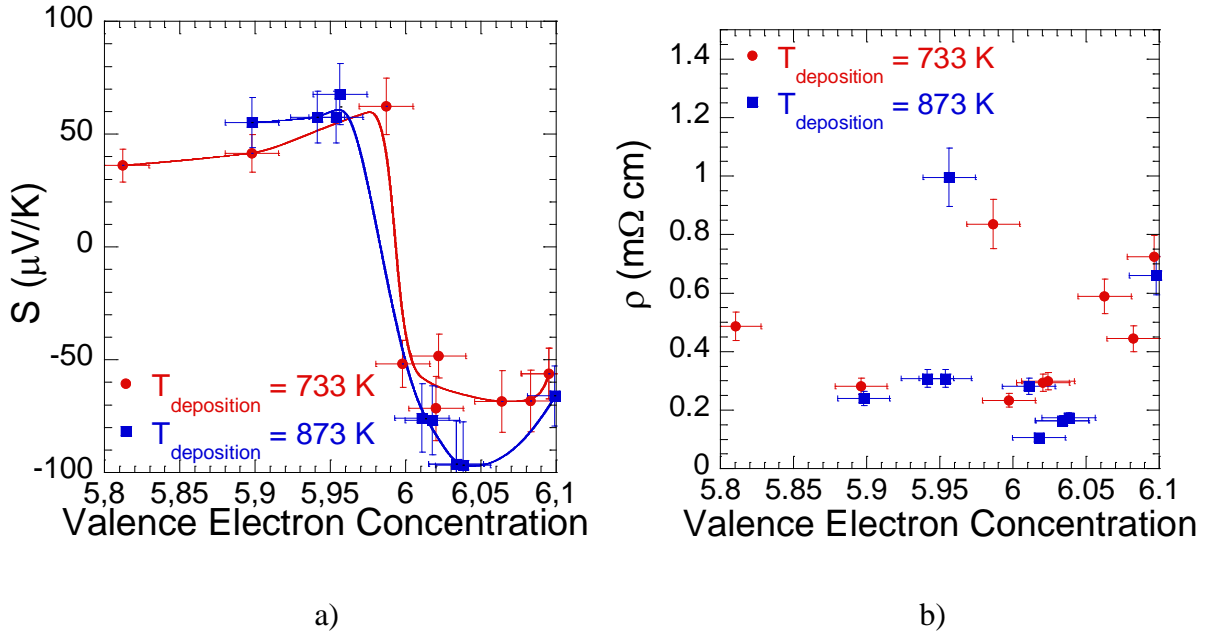


**Figure 4 : Seebeck coefficient (a) and electrical resistivity (b) versus valence electron concentration (VEC) calculated from atomic concentration analysis.**

### 3.3 Power factor versus valence electron concentration and charge carrier concentration

Figure 5 shows the power factor  $P_F$  versus VEC for films deposited at 733 K (in red) and 873 K (in blue). For  $p$ -type thin films ( $VEC < 6$ ), the power factor is weakly dependent on the deposition temperature, with a maximum of  $1.3 \text{ mW}/\text{K}^2\text{m}$ . The effect is more prominent for  $n$ -type films: high values up to  $5.6 \text{ mW}/\text{K}^2\text{m}$  are obtained for these films deposited at 873 K. This high power factor has been obtained in a film with  $\text{Fe}_{49.2}\text{V}_{28.7}\text{Al}_{22.1}$  as EDX atomic film composition ( $\text{Fe}_{1.97}\text{V}_{1.15}\text{Al}_{0.88}$ ), sputtered by applying 134 W and 17W to the principal  $\text{Fe}_2\text{VAl}$  and secondary V targets respectively. It should be mentioned that such results constitute a current record for thin films in the Fe-V-Al system, since the  $P_F$  value obtained in reference <sup>21</sup> has not yet been reproduced. It can be surmised that the good performances found in films deposited at 873 K are related to their high crystalline order. This high deposition temperature most likely cures the microstrains induced by the MgO substrate that could lead to disordering from its ideal  $L2_1$  structure, as already reported and discussed in reference <sup>26</sup>. These microstrain effects are clearly visible in figure S2 in supporting information showing the grain sizes and grain boundaries quality for different temperature deposition. At 873 K, the grains become invisible, showing that the grain boundaries are of excellent quality, whereas they are clearly visible at lower deposition temperature.

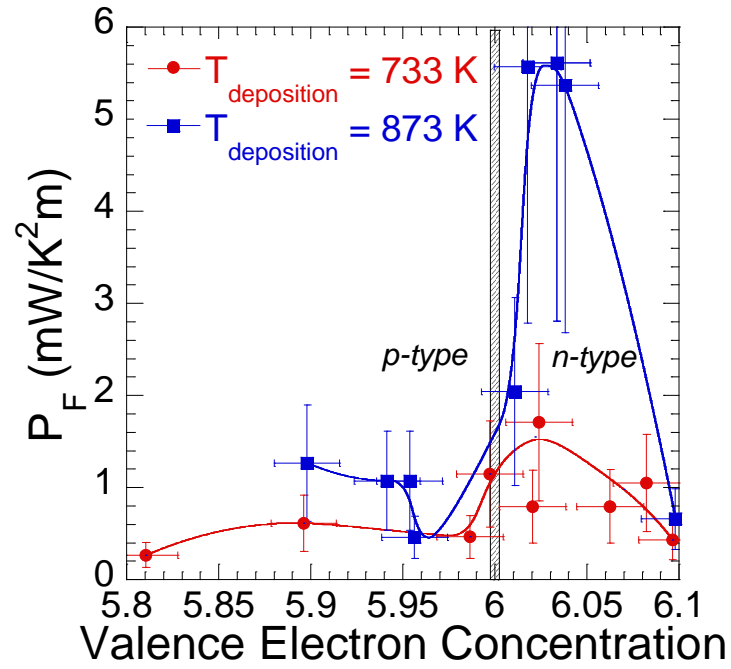


**Figure 5 : Power factor versus valence electron concentration for films deposited at 733 K (in red) and 873 K (in blue).**

Carrier concentration was measured at 300 K on *n*-type and *p*-type films deposited at 733 and 873 K. Table 1 shows carrier concentration, mobility, electrical resistivity and  $P_F$  for different values of VEC. For  $VEC < 6$ , thin films display a *p*-type conduction with a concentration of 2.8 and 4.7  $10^{21}$  holes  $\text{cm}^{-3}$  as majority charge carriers. V-rich compositions ( $VEC > 6$ ) leads to *n*-type conduction with carrier concentrations larger than those obtained for *p*-type films. For the *n*-type film showing the highest  $P_F$ ,  $n$  is close to  $-10^{22}$   $\text{cm}^{-3}$ . This high value remains within the range of carrier concentrations obtained in the literature on  $\text{Fe}_{2+x}\text{V}_{1+y}\text{Al}_{1+z}$ , showing power factor ranging from 2 to 7.6  $\text{mW m}^{-1} \text{K}^{-2}$ .<sup>5,27</sup>

Sample VEC	$T_{\text{deposition}}$ (K)	$S$ ( $\mu\text{V}/\text{K}$ ) +/-20%	$\rho$ ( $\text{m}\Omega \text{ cm}$ ) +/-10%	$n/p$ ( $10^{21} \text{ cm}^{-3}$ ) +/-10%	$\mu$ ( $\text{cm}^2/\text{Vs}$ ) +/-20%	$P_F$ ( $\text{mW}/\text{K}^2\text{m}$ ) +/-50%
5.81	733	36	0.486	2.8	4.6	0.3
5.90	873	55	0.240	3.4	7.8	1.3
5.94	873	57	0.309	4.7	4.3	1.1
5.96	873	68	0.996	2.7	2.3	0.5
5.99	733	62	0.836	3.9	1.9	0.5
6.01	873	-76	0.281	-7.7	-2.9	2.0
6.02	733	-72	0.299	-9.7	-2.2	1.7
6.03	873	-96	0.165	-11.0	-3.4	5.6

6.06	733	-68	0.589	-7.7	-1.4	0.8
------	-----	-----	-------	------	------	-----

**Table 1 :VEC and electronic transport properties of thin films deposited at 733 K (in red) and 873 K (in blue). The black line corresponds to the transition from p-type to n-type films.**

### 3.4 Substrate effect on electronic transport properties

Fe-V-Al magnetron sputtering was tested on single crystalline YSZ, NdGaO<sub>3</sub>, MgO and Si and amorphous SiO<sub>2</sub> and SiN substrates because Fe<sub>2</sub>VAl thin films could be deposited on different types of substrates, depending on the envisaged applications. Substrate influence on the microstructure and electronic transport properties was thus studied.

Figure 6 shows X ray diffraction patterns for Fe-V-Al films deposited on these different substrates at 873 K. For single crystalline MgO, YSZ and NdGaO<sub>3</sub> substrates, films show a preferred orientation growth. Peaks corresponding to single crystalline substrate are very intense and clearly visible in figure 6a. X ray diffraction pattern magnification in Supporting Information (Figure S3) shows an epitaxial growth respectively along the (220) and (200) orientation for YSZ and MgO substrates. For NdGaO<sub>3</sub> substrate, the epitaxy is not perfect, but a preferred orientation is observed along the (200) direction. As shown in figure 6b, films grown on amorphous SiO<sub>2</sub> substrate show no grain orientation and the presence of the (111) and (311) peaks corresponding to the L<sub>21</sub> phase should be noticed.

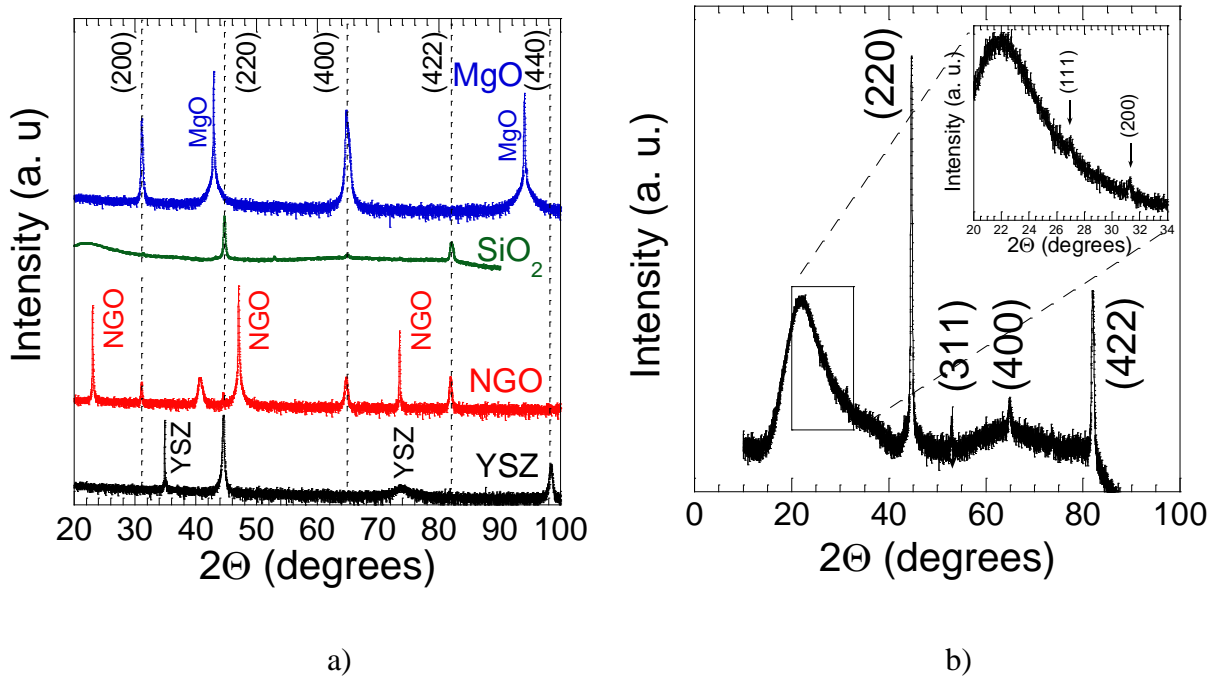


**Figure 6 : a) X ray diffraction patterns plotted with log intensity scale for films deposited on YSZ, NdGaO<sub>3</sub>, SiO<sub>2</sub> and MgO substrates. b) X ray diffraction pattern for films deposited on SiO<sub>2</sub> substrates. Pattern in the 20 - 34 degrees range is shown in inset.**

Table 2 summarizes film deposition conditions and electronic transport properties obtained on the six substrates with the same plasma and temperature deposition conditions. It can be noticed that films deposited on SiO<sub>2</sub>, Si and SiN substrates were not measurable because of a low adherence. In contrast the  $S$ ,  $\rho$  and  $P_F$  values are similar, ranging from 4.6 to 5.3 mW/K<sup>2</sup>m for films obtained on YSZ, NdGaO<sub>3</sub> and MgO substrates. Electrical resistivity is the same for the three samples. Thin films deposited on YSZ, NdGaO<sub>3</sub> substrates display a n-type conduction with a concentration of respectively  $-8 \times 10^{21}$  and  $-9.5 \times 10^{21}$  electron cm<sup>-3</sup> as majority charge carriers. These values are close to those obtained in thin films deposited on MgO with the same deposition conditions ( $-1.1 \times 10^{22}$  electron cm<sup>-3</sup>). Although such small differences fall within  $P_F$  measurement uncertainty, it can also be attributed to the microstrain induced in the film by the YSZ and NdGaO<sub>3</sub> substrates because of the differing lattice parameters or thermal expansion coefficients.

Sample	Substrate	Fe <sub>2</sub> VAl/Al/V Plasma power (W)	T <sub>deposition</sub> (K)	S ( $\mu$ V/K) +/-20%	Thickness (nm) +/-10%	$\rho$ (m $\Omega$ cm) +/-10%	$n$ (10 <sup>21</sup> cm <sup>-3</sup> ) +/-10%	$P_F$ (mW/K <sup>2</sup> m) +/-50%
SE30 <sub>1</sub>	YSZ	135/0/15	873	-91	500	0.177	-8.0	4.6
SE30 <sub>2</sub>	NdGaO <sub>3</sub>	135/0/15	873	-88	500	0.168	-9.5	4.6
SE30 <sub>3</sub>	SiO <sub>2</sub>	135/0/15	873	-	500	-	-	-
SE30 <sub>4</sub>	MgO	135/0/15	873	-97	500	0.174	-11.0	5.3
SE33 <sub>3</sub>	SiN	134/24/0	873	-	460	-	-	-
SE32 <sub>1</sub>	Si	134/0/17	873	-	500	-	-	-

**Table 2: Deposition conditions and electronic transport properties of thin films deposited on different substrates.**

Figure 7 shows the FESEM surface morphologies of films deposited at 873 K on these six substrates. The growth is epitaxial for single crystalline substrates such as YSZ, NdGaO<sub>3</sub> and MgO. Grain and grain boundaries are visible with square like shape grain growth following the [110] direction of the substrate, except for MgO where epitaxial growth is perfect at 873 K deposition, leading to a single crystalline film. For non-single crystal substrates such as Si, SiO<sub>2</sub> and SiN, grain size is around a few hundred nanometers with no

preferred orientation, and the visible cracks explain the difficulty in carrying out transport measurements. These cracks, or adhesion problems, are due to thermal expansion differences between the substrate and the deposited film. It should also be mentioned that the large thickness of deposited films can also induce strain and might crack in the films. In the future, it is planned to study the deposition of  $\text{Fe}_2\text{VAl}$  on intermediate or “buffer” layers such as  $\text{MgO}$ , to grow films of good quality while promoting adherence on non-single-crystalline substrates and to study the influence of the film thickness on the cracks.

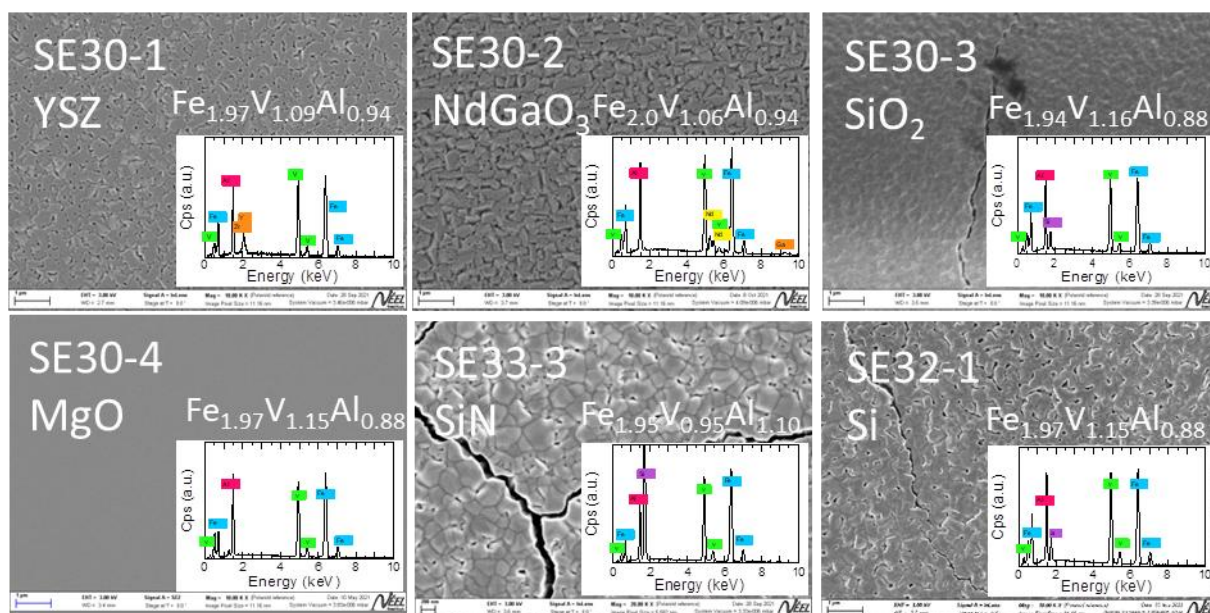


**Figure 7 : FESEM micrographs taken in secondary electron imaging (SEI) mode on films deposited on different substrates at 873 K. EDX spectrum and composition analysis are enclosed in inset.**

### 3.5 Annealing treatments

Film annealing was carried out in a tube furnace under secondary vacuum close to  $10^{-6}$  mbar for a film deposited at 733 K. Four successive temperatures were chosen:  $T_{\text{annealing}} = 873$  K, 923 K, 973 K and 1023 K for a constant duration of 15 hours. The atomic film composition after deposition was  $\text{Fe}_{48.4}\text{V}_{30.1}\text{Al}_{21.5}$ . The Seebeck coefficient and power factor before annealing were respectively  $-48 \mu\text{V/K}$  and  $0.8 \text{ mW/K}^2\text{m}$  with a VEC of 6.02.

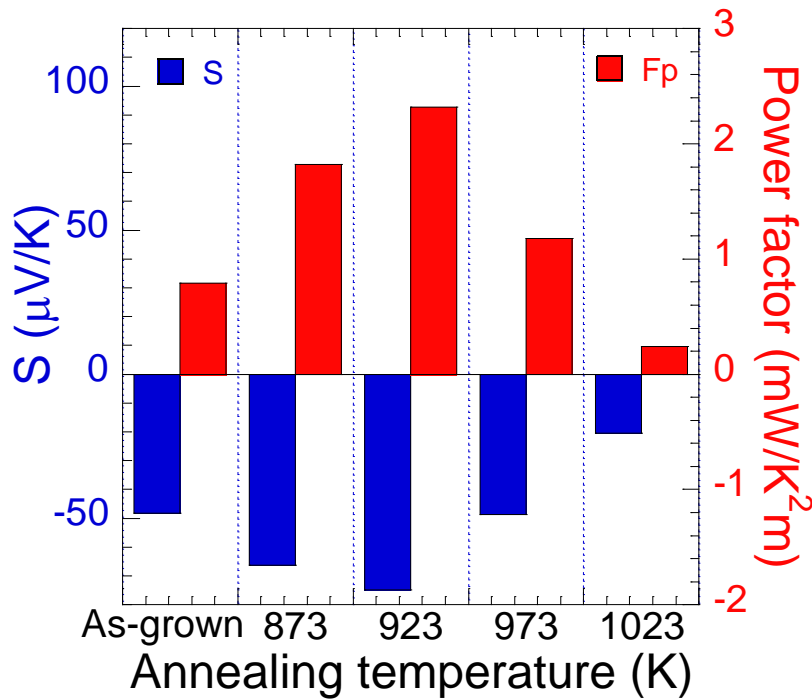


**Figure 8 : Seebeck coefficient and power factor for different annealing temperatures.**

Figure 8 shows variation of the Seebeck coefficient and power factor as a function of the annealing temperature. We observe an increase of the Seebeck coefficient from -48 to -75  $\mu\text{V/K}$  up to 923 K, followed by a sharp decrease beyond 973 K. Similarly, the power factor is increased by a factor of 3 when annealing at 923 K: it increases from 0.8 to 2.3  $\text{mW/K}^2\text{m}$ . Beyond 923 K, annealing leads to a decrease of  $P_F$ . FESEM micrographs taken in secondary electron imaging (SEI) mode on films annealed at 1023 K reveal a crystal growing along two perpendicular directions (See Figure S4a in Supporting Information). At the film surface, 200 – 300 nm size grains with a poor iron (47 at%) and rich vanadium (30 at%) composition are clearly present. It is difficult to interpret this result as the  $\text{Fe}_2\text{VAl}$  phase is stable up to 1353 K<sup>26</sup> and should not transform into another phase. We do not understand this phenomenon yet and will further investigate the reason for this Seebeck coefficient decay in a future work, and its possible correlation to a phase change.

#### 4-Discussion

A high power-factor for  $n$ -type thin films is obtained in a very narrow  $VEC$  window (6.01-6.04). To our best knowledge, this  $P_F$  dependence with  $VEC$  was not observed before. On the other hand, the dependence for the Seebeck coefficient (Figure 3) is similar to what has been previously observed by several authors.<sup>28,29</sup> For co-sputtered samples using

vanadium target with a  $VEC \geq 6$ , the Seebeck coefficient becomes negative with the formation of  $n$ -type films. Values close to  $-100 \mu\text{V/K}$  are obtained for the best films. For co-sputtered samples using the secondary aluminum target with  $VEC < 6$ , the Seebeck coefficient is positive ranging from  $+35 \mu\text{V/K}$  to  $+68 \mu\text{V/K}$  and giving rise to  $p$ -type conduction. Such low Seebeck values found for  $p$ -type in this work are comparable to literature values for either thin films or bulk  $p$ -type materials. Indeed, the groups of Nishino<sup>28</sup> and Mikami<sup>29</sup> measured Seebeck coefficients close to  $95 \mu\text{V/K}$  at 350 K in their bulk  $p$ -type  $\text{Fe}_2\text{V}_{1-x}\text{Al}_{1+x}$  alloys, smaller than the  $-145 \mu\text{V/K}$  reached in  $n$ -type. The larger Seebeck coefficient for  $n$ -type conduction is attributed to a larger effective mass for the electrons than for the holes. Electronic transport optimization of  $p$ -type thermoelectric alloys or thin films remains a challenge. Substitution with a fourth chemical element needs to be investigated in further work.

The  $P_F$  values are higher for the films elaborated at 873 K, because mobilities are globally higher than for the films elaborated at 733 K (see table 1). At 733 K the microstructure presents very marked grain boundaries inducing high electrical resistivity. Moreover, at this deposition temperature, compositions crystallize in the A2 structure rather than in the desired ordered  $\text{L2}_1$  as observed in the literature.<sup>30,31</sup>

To our best knowledge, the power factor obtained in this work ( $5.6 \text{ mW/K}^2\text{m}$ ) is higher than most of the values found for thin film in the literature, except for the unexpectedly large value of  $P_F = 50 \text{ mW m}^{-1} \text{ K}^{-2}$  obtained by Hinterleitner et al at 350 K in a  $\text{Fe}_2\text{V}_{0.8}\text{W}_{0.2}\text{Al}$  thin film.<sup>21</sup> A value of  $3.0 \text{ mW/K}^2\text{m}$  was obtained at 323 K for  $\text{Fe}_{1.93}\text{V}_{1.05}\text{Al}_{0.77}\text{Si}_{0.24}$  by Fukatani et al<sup>11</sup> for a 300K film deposition and post annealing at 1073 K. Film composition was controlled for the Fe-poor and V-rich off-stoichiometric composition by introducing elemental chips on the sputtering target, resulting in  $VEC$  variations ranging from 5.9 to 6.1. In another work, Furuta et al<sup>13</sup> published a maximum magnitude of the Seebeck coefficient which was less than  $30 \mu\text{V/K}$ , with electrical resistivity between  $0.9 - 1.2 \text{ m}\Omega - \text{cm}$  at 300 K. A  $P_F$  value of  $2.3 \text{ mW/K}^2\text{m}$  measured at around 340 K has been reached by Hiroi et al. for a film deposited at 1073 K.<sup>17</sup> It corresponds to twice the maximum power factor obtained at 350 K by Mikami et al.<sup>12</sup> in Ti-substituted  $\text{Fe}_2\text{VAl}$  thin films, and at 300 K by Kudo et al. in  $\text{Fe}_{2-x}\text{V}_{1+x}\text{Al}$  films grown by MBE technique.<sup>19</sup> It should be mentioned that our results are close to the highest values obtained in  $\text{Fe}_2\text{VAl}$  based alloys in bulk state with  $P_F = 7.6 \text{ mW/K}^2\text{m}$  recently obtained at 300 K in a 1653 K - quenched stoichiometric  $\text{Fe}_2\text{VAl}$  sample<sup>5</sup>

or  $P_F = 6.7 \text{ mW/K}^2\text{m}$  reported in bulk  $n$ -type  $\text{Fe}_{1.98}\text{V}_{1.02}\text{Al}_{0.9}\text{Si}_{0.1}$ <sup>6</sup> at 300 K and  $\text{Fe}_2\text{V}_{1.03}\text{Al}_{0.97}$ <sup>4</sup> at 250 K.

## 5-Conclusion

Heusler-type  $\text{Fe}_2\text{VAl}$  thin films were developed using various deposition conditions with a co-sputtering process enabling film composition tuning. The best power factor obtained for the  $n$ -type conduction reaches  $5.6 \text{ mW/K}^2\text{m}$  for a 873 K deposition temperature, thanks to a high Seebeck factor value of  $-97 \mu\text{V/K}$  and a low resistivity of  $0.17 \text{ m}\Omega\cdot\text{cm}$ . For  $p$ -type conduction, the best power factor is  $1.4 \text{ mW/K}^2\text{m}$  and the Seebeck coefficient obtained in this case is only  $+57 \mu\text{V/K}$ . Such  $P_F$  values need further investigation and process optimization.

## Supporting Information

Thickness homogeneity measurements of  $\text{Fe}_2\text{VAl}$  thin films, effect of the deposition temperature on the grain size and grain boundaries, complement of the X ray diffraction study and FESEM micrographs taken on films annealed at 1023 K.

## Acknowledgement

This work has been partially funded by the CNRS Energy unit through the project COMITHER (n° EDP121268) and by the “Agence Nationale de la Recherche” through the contract “LoCoThermH” (Project ANR-18-CE05-0013-01). The authors thank N. Caillault and S. Giraud from Schneider Electric for profilometer measurements. They also thank mechanical facilities of Institut Néel - CNRS: the Pôle Cryogénique (A. Gerardin) and SERAS (S. Garcia, G. Perroux) for sample holder fabrication and target cutting.

## References

- [1] Nishino, Y. Development of Thermoelectric Materials Based on  $\text{Fe}_2\text{VAl}$  Heusler Compound for Energy Harvesting Applications. IOP Conf. Ser.: Mater. Sci. Eng. 2011, 18, 142001 /1–6.
- [2] Galanakis, I.; Dederichs, P. H.; Papanikolaou, N. Slater-Pauling Behavior and Origin of the Half-Metallicity of the Full-Heusler Alloys. Phys. Rev. B 2002, 66, 174429/1-9.

- [3] Miyazaki, H.; Tanaka, S.; Ide, N.; Soda, K.; Nishino, Y. Thermoelectric Properties of Heusler-Type Off-Stoichiometric  $\text{Fe}_2\text{V}_{1+x}\text{Al}_{1-x}$  Alloys. *Mater. Res. Express* 2014, 1, 015901/1-9.
- [4] Diack-Rasselio, A.; Rouleau, O.; Coulomb, L.; Georgeton, L.; Beaudhuin, M.; Crivello, J.-C.; Alleno, E. Influence of Self-Substitution on the Thermoelectric  $\text{Fe}_2\text{VAl}$  Heusler Alloy. *J. Alloys Compd.* 2022, 920, 166037/1-10.
- [5] Garmroudi, F.; Parzer, M.; Riss, A.; Ruban, A.; Khmelevskiy, S.; Reticcioli, M.; Knopf, M.; Michor, H.; Pustogow, A.; Mori, T.; Bauer, E. Anderson Transition in Stoichiometric  $\text{Fe}_2\text{VAl}$ : High Thermoelectric Performance from Impurity Bands. *Nat. Commun.* |2022, 13, 3599/1-10.
- [6] Nishino, Y.; Tamada, Y. Doping Effects on Thermoelectric Properties of the Off-Stoichiometric Heusler Compounds  $\text{Fe}_{2-x}\text{V}_{1+x}\text{Al}$ . *J. Appl. Phys.* 2014, 115, 123707/1-8.
- [7] Kawaharada, Y.; Kurosaki, K.; Yamanaka, S. Thermophysical Properties of  $\text{Fe}_2\text{VAl}$ . *J. Alloys Compd.* 2003, 352/48-52.
- [8] Alleno, E. Review of the Thermoelectric Properties in Nanostructured  $\text{Fe}_2\text{VAl}$ . *Metals* 2018, 8, 864/1-7.
- [9] Renard, K.; Mori, A.; Yamada, Y.; Tanaka, S.; Miyazaki, H.; Nishino, Y. Thermoelectric Properties of the Heusler-type  $\text{Fe}_2\text{VTa}_x\text{Al}_{1-x}$  Alloys. *J. Appl. Phys.* 2014, 115, 033707/1-7.
- [10] Masuda, S.; Tsuchiya, K.; Qiang, J.; Miyazaki, H.; Nishino, Y. Effect of High-Pressure Torsion on the Microstructure and Thermoelectric Properties of  $\text{Fe}_2\text{VAl}$ -Based Compounds. *J. Appl. Phys.* 2018, 124, 035106/1-9.
- [11] Fukatani, N.; Kurosaki, Y.; Yabuuchi, S.; Nishide, A.; Hayakawa, J. Improved Power Factor in Low Thermal Conductive  $\text{Fe}_2\text{VAl}$ -Based Full-Heusler Thin Films by Composition-Control with Off-Axis Sputtering Method. *Appl. Phys. Lett.* 2018, 112, 033902/1-4.
- [12] Mikami, M.; Kamiya, T.; Kobayashi, K. Microstructure and Thermoelectric Properties of Heusler  $\text{Fe}_2\text{VAl}$  Thin-Films. *Thin Solid Films* 2010, 518, 2796-2008.
- [13] Furuta, Y.; Kato, K.; Miyawaki, T.; Asano, H.; Takeuchi, T.  $\text{Fe}_2\text{VAl}$ -Based Thermoelectric Thin Films Prepared by a Sputtering Technique. *J. Electron. Mater.*, 2014, 43, 2157-2164.
- [14] Nishide, A.; Kurosaki, Y.; Yamamoto, H.; Yabuuchi, S.; Okamoto, M.; Hayakawa, J. Thermoelectric Properties of Full-Heusler Type  $\text{Fe}_2\text{VAl}$  Thin Films. *J. Jpn. Inst. Met.* 2012, 76, 541-545.
- [15] Gao, W.; Liu, Z.; Baba, T.; Guo, Q.; Tang, D.; Kawamoto, N.; Bauer, E.; Tsujii, N.; Mori, T. Significant Off-Stoichiometry Effect Leading to the N-Type Conduction and

Ferromagnetic Properties in Titanium Doped Fe<sub>2</sub>VAl Thin Films. *Acta Mater.* 2020, 200, 848-856.

[16] Kurosaki, Y.; Yabuuchi, S.; Nishide, A.; Fukatani, N.; Hayakawa, J. Crystal Growth and Flat-Band Effects on Thermoelectric Properties of Fe<sub>2</sub>TiAl-Based Full-Heusler Thin Films. *AIP Adv.* 2020, 10, 115313/1-6.

[17] Hiroi, S.; Mikami, M.; Takeuchi, T. Thermoelectric Properties of Fe<sub>2</sub>VAl-Based Thin-Films Deposited at High Temperature. *Mater. Trans.* 2016, 57, 1628-1632.

[18] Hiroi, S.; Nishino, S.; Choi, S.; Seo, O.; Kim, J.; Chen, Y.; Song, C.; Tayal, A.; Sakata, O.; Takeuchi, T. Phonon Scattering at the Interfaces of Epitaxially Grown Fe<sub>2</sub>VAl/W and Fe<sub>2</sub>VAl/Mo Superlattices. *J. Appl. Phys.* 2019, 125, 225101/1-7.

[19] Kudo, K.; Yamada, S.; Chikada, J.; Shimanuki, Y.; Nakamura, Y.; Hamaya, K. Effect of Fe–V Nonstoichiometry on Electrical and Thermoelectric Properties of Fe<sub>2</sub>VAl Films. *Jpn. J. Appl. Phys.* 2018, 57, 040306/1-4.

[20] Yamada, S.; Kudo, K.; Okuhata, R.; Chikada, J.; Nakamura, Y.; Hamaya, K. Low Thermal Conductivity of Thermoelectric Fe<sub>2</sub>VAl Films. *Appl. Phys. Express* 2017, 10, 115802/1-4.

[21] Hinterleitner, B.; Knapp, I.; Ponder, M.; Shi, Y.; Müller, H.; Eguchi, G.; Eisenmenger-Sittner, C.; Stöger-Pollach, M.; Kakefuda, Y.; Kawamoto, N.; Guo, Q.; Baba, T.; Mori, T.; Ullah, S.; Chen, X.-Q.; Bauer, E. Thermoelectric Performance of a Metastable Thin-Film Heusler Alloy. *Nature* 2019, 576, 85-90.

[22] Mikami, M.; Kinemuchi, Y.; Ozaki, K.; Terazawa, Y.; Takeuchi, T. Thermoelectric Properties of Tungsten-Substituted Heusler Fe<sub>2</sub>VAl Alloy. *J. Appl. Phys.* 2012, 111, 093710/1-6.

[23] Bourgault, D.; Giroud-Garampon, C.; Caillault, N.; Carbone, L.; Aymami, J.A. Thermoelectric Properties of n-Type Bi<sub>2</sub>Te<sub>2.7</sub>Se<sub>0.3</sub> and p-Type Bi<sub>0.5</sub>Sb<sub>1.5</sub>Te<sub>3</sub> Thin Films Deposited by Direct Current Magnetron Sputtering. *Thin Solid Films* 2008, 516, 8579-8583.

[24] Nishino, Y.; Kato, M.; Asano, S.; Soda, K.; Hayasaki, M.; Mizutani, U. Semiconductorlike Behavior of Electrical Resistivity in Heusler-type Fe<sub>2</sub>VAl Compound. *Phys. Rev. Lett.* 1997, 79, 1909-1912.

[25] Nishino Y.; Kumada C.; Asano S. Phase Stability of Fe<sub>3</sub>Al with Addition of 3d Transition Elements, *Scr. Mater.* 1997, 36, 461–466.

[26] Maier, S.; Denis, S.; Adam, S.; Crivello, J.-C.; Joubert, J.-M.; Alleno, E. Order-Disorder Transitions in the Fe<sub>2</sub>VAl Heusler Alloy. *Acta Mater.* 2016, 121, 126-136.

- [27] Parzer, M.; Garmroudi, F.; Riss, A.; Khmelevskiy, S.; Mori, T.; Bauer, E. High Solubility of Al and Enhanced Thermoelectric Performance Due to Resonant States in  $\text{Fe}_2\text{VAl}_x$ . *Appl. Phys. Lett.* 2022 120, 071901/1-7.
- [28] Nishino, Y.; Kamizono, S.; Miyazaki, H.; Kimura, K. Effects of Off-Stoichiometry and Ti Doping on Thermoelectric Performance of  $\text{Fe}_2\text{VAl}$  Heusler Compound. *AIP Adv.* 2019, 9, 125003/1-7.
- [29] Mikami, M.; Inukai, M.; Miyazaki, H.; Nishino, Y. Effect of Off-Stoichiometry on the Thermoelectric Properties of Heusler-Type  $\text{Fe}_2\text{VAl}$  Sintered Alloys. *J. Electron. Mater.* 2015, 45 1284-1289.
- [30] Masuda, S.; Tsuchiya, K.; Qiang, J.; Miyazaki, H.; Nishino, Y. Effect of High-Pressure Torsion on the Microstructure and Thermoelectric Properties of  $\text{Fe}_2\text{VAl}$ -Based Compounds. *J. Appl. Phys.* 2018, 124 035106/1-9.
- [31] Diack-Rasselio A. Optimisation et Nanostructuration de l'Alliage d'Heusler Thermoélectrique  $\text{Fe}_2\text{VAl}$ . Doctoral dissertation, Université Paris-Est Créteil Val de Marne, France, 2022.